Effect of Road Quality in Structural Health Monitoring under Operational Conditions

Vesna Jaksic[1], Vikram Pakrashi[1], Alan O'Connor[2]
[1]Department of Civil and Environmental Engineering, University College Cork, College Road, Cork, Ireland
[2]Department of Civil, Structural and Environmental Engineering, Trinity College Dublin, College Green, Dublin 2, Ireland
email: v.jaksic@umail.ucc.ie, V.Pakrashi@ucc.ie, alan.oconnor@tcd.ie

ABSTRACT: The effect of unevenness in a bridge deck for the purpose of Structural Health Monitoring (SHM) under operational conditions is studied in this paper. The moving vehicle is modelled as a single degree of freedom system traversing the damaged beam at a constant speed. The bridge is modelled as an Euler-Bernoulli beam with a breathing crack, simply supported at both ends. The breathing crack is treated as a nonlinear system with bilinear stiffness characteristics related to the opening and closing of crack. The unevenness in the bridge deck considered is modelled using road classification according to ISO 8606:1995(E). Numerical simulations are conducted considering the effects of changing road surface classes from class A – very good to class E – very poor. Cumulant based statistical parameters, based on a new algorithm are computed on stochastic responses of the damaged beam due to passages of the load in order to calibrate the damage. Possibilities of damage detection and calibration under benchmarked and non-benchmarked cases are considered. The findings of this paper are important for establishing the expectations from different types of road roughness on a bridge for damage detection purposes using bridge-vehicle interaction where the bridge does not need to be closed for monitoring.

KEY WORDS: Structural Health Monitoring (SHM); Euler–Bernoulli Beam; Open Crack; Road Surface.

1 INTRODUCTION

Structural Health Monitoring (SHM) is an integral part of infrastructure maintenance management. Non-destructive structural damage detection, in this regard, is becoming an important aspect of integrity assessment for aging, extreme-event affected or inaccessible structures [1-3]. A damage in a structure often tend to change only the local dynamic characteristics and markers of damage detection should attempt to capture such local dynamic changes. In this regard, employing bridge–vehicle interaction models for damage detection [4] and SHM [5-7] has gained considerable interest in recent times

Bilello and Bergman [8] have considered, theoretically and experimentally, the response of smooth surface damaged Euler–Bernoulli beam traversed by a moving mass, where the damage was modelled through rotational springs. Bu et al. [9] have proposed damage assessment approach from the dynamic response of a passing vehicle through a damage index. Poor road surface roughness was observed to be a bad detector for damage in their approach. Majumder and Manohar [10] have proposed time domain damage descriptor to reflect the changes in bridge behavior due to damage. Lee et al. [11] have experimentally investigated the possible application of bridge–vehicle interaction data for identifying the loss of bending rigidity. Law and Zhu [12] have studied the dynamic behavior of damaged reinforced concrete bridge under moving loads using a model of a simply supported beam with open and breathing cracks. Pakrashi et al. [4] have performed experimental investigation of simply supported beam with moving load subjected to different level of damage.

Local damage in beams have been modelled in a number of ways [13]. Narkis [14] has proposed a method for calculation of natural frequencies of a cracked simply supported beam using an equivalent rotational spring. Sundermeyer and Weaver [15] have exploited the non-linear character of vibrating beam with a breathing crack. The surface roughness on bridges has never been used as an aid to damage detection.

This paper proposes the use of changing road surface roughness in damage detection of beam-like structures through bridge vehicle interaction and investigates what road quality is appropriate for such detection. Harris et al [16] have proposed a method for characterisation of pavement roughness through the analysis of vehicle acceleration. Fryba [17] has shown the effect of road surface roughness (RSR) on bridge response. Abdel-Rohman and Al-Duaij [18] investigated the effects of unevenness in the bridge deck on the dynamic response of a single span bridge due to moving loads. O'Brien et al. [19] have proposed a bridge roughness index (BRI) which gives insight into the contribution that road roughness makes to dynamics of simply supported bridges. Da Silva [20] has proposed a methodology to evaluate the dynamical effects, displacement and stress on highway bridge decks due to vehicle crossing on rough pavement surfaces. Although there are many interesting numerical and statistical markers and methods available for damage detection [21-24], surface roughness has always been treated for parameter studies, improved analysis or for establishing the bounds of

efficiency of an algorithm. Jaksic et al. [25] have very recently investigated the potential of using surface roughness for detecting damage where a white noise excitation response of a single degree of freedom bilinear oscillator was investigated. The white noise represented a broadband excitation, qualitatively similar to the interaction with surface roughness and the bilinearity attempted to capture a breathing crack. First and second order cumulants of the response of this system were observed to be appropriate markers for detecting changes in system stiffness.

In this paper a beam-vehicle interaction based damage detection from multiple point observations in the time domain using the interaction with realistic surface roughness is presented. The damage has been modelled as a localized breathing crack and surface roughness has been defined by ISO 8606:1995 [26]. The first mode of undamaged and damaged beam and their first time derivatives are considered [22, 27] along the length at a number of equidistant points. These are relatively easier to estimate and are often a good approximation of the actual displacement or velocity. The preferable road quality for damage detection process is investigated in considerable details in this paper.

2 METHODOLOGY

2.1 Model

The bridge is represented as a simply supported Euler-Bernoulli beam with a breathing crack traversed by a single degree of freedom oscillator (Figure 1), which represents the vehicle. The vehicle is assumed to be moving on the surface without losing contact. The length of the beam is L and the crack is at a distance x_c from the left support. The beam has a constant cross-sectional area A, second moment of area I, Young's modulus E and mass density ρ. The crack can be modelled as a rotational spring [15] when the crack is open.

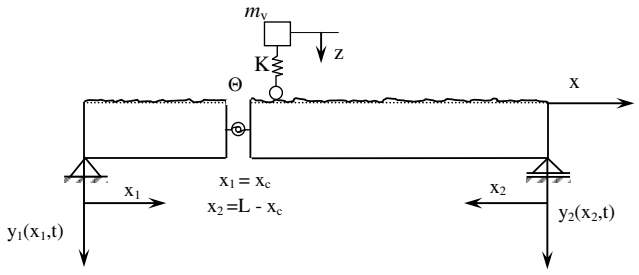

Figure 1. Simply supported beam with breathing crack modelled as two beams connected by torsional spring

2.2 Equations of motion

The equation of motion of a beam with a breathing crack and traversed by a vehicle is given as

$$EI\frac{\partial^4 y_i(x,t)}{\partial x^4} + c\frac{\partial y_i(x,t)}{\partial t} + \rho A\frac{\partial^2 y_i(x,t)}{\partial t^2} = P\delta(x - \upsilon t);\ i = 1,2 \quad (1)$$

t is the time coordinate with the origin at the instant of the force arriving upon the beam; x is the length coordinate with the origin at the left-hand end of the beam; $y_i(x,t)$ is the transverse deflection of the beam at the point x and time t, measured from the static equilibrium position corresponding to when the beam is loaded under its own weight; c is the structural damping of the material of the beam; $m = \rho A$ is the mass per unit length; P is the external force; δ is the Dirac Delta function [17] and υt is the position of the vehicle moving with constant speed υ from left support. The external force P is defined as:

$$P = \{m_V g + K[z - y_i(\upsilon t, t) - r(\upsilon t)]\};\quad i = 1,2 \quad (2)$$

$$K[z - y_i(\upsilon t, t) - r(\upsilon t)] \geq 0 \quad (3)$$

where m_v is the mass of the vehicle; g is acceleration due to gravity; K is the equivalent stiffness of the vehicle's tires and springs; z is the vertical displacement of the vehicle with respect to its static equilibrium position; and r is the surface roughness.

2.2.1 The open crack eigenvalue problem

When the crack is open, the system consists of two beams connected by torsional spring, where each continuous segment of the beam can be described by the Bernoulli-Euler partial differential equation of motion. The eigenvalue problem can be solved through the method of separation of variables and the consideration of modal superposition:

$$y_i(x\ ,t) = \sum_{j=0}^{n} \phi_j^i(x\ )\, q_j(t);\quad i = 1,2 \quad (4)$$

where Φ_i is orthogonal mode shape for the i[th] mode and q_i is the time dependent amplitude. By separating temporal and spatial variables, the following differential equation system is obtained

$$\phi_i^{i\prime\prime\prime\prime}(x\ ) - \frac{\omega_j^2\ \rho A}{EI}\phi_j^i(x\ ) = 0;\quad i = 1,2;\ j = 1\ to\ n \quad (5)$$

$$\ddot{q}_j(t) + \omega_j^2 q_j(t) = 0;\quad j = 1\ to\ n \quad (6)$$

There are no displacements or moments at the supports. Also, boundary conditions at the crack location x_c must satisfy continuity of displacement, bending moment and shear and the slope between the two beam segments can be related to the moment at this section [15]. The solution of the spatial differential equation (5) satisfying all eight boundary conditions is:

$$0 < \bar{x} < x_c \rightarrow\quad \phi = A_0(\sin a\bar{x} + \alpha \sinh a\bar{x}) \quad (7)$$

$$x_c < \bar{x} < L\ \rightarrow$$

$$\phi = A_0\left(\frac{\sin(ax_c)\sin(a(L-\bar{x}))}{\sin(a(L-x_c))} + \alpha\frac{\sinh(ax_c)\sinh(a(L-\bar{x}))}{\sinh(a(L-x_c))}\right) \quad (8)$$

where:

$$a^4 = \frac{\omega_j^2 \rho A}{EI};\ \ j = 1\ to\ n \quad (9)$$

$$\alpha = \frac{\cos ax_c + \frac{\sin ax_c}{\tan a(L-x_c)}}{\cosh ax_c + \frac{\sinh ax_c}{\tanh a(L-x_c)}} \quad (10)$$

and the constant A_0 is chosen so that the mode shapes are normalized as

$$\int_0^{x_c}(\phi_j(\bar{x}))^2 d\bar{x} + \int_{x_c}^{L}(\phi_j(\bar{x}))^2 d\bar{x} = 1 \quad (11)$$

The natural frequencies of the beam with the open crack can be calculated replacing boundary conditions in assumed solution of mode shape equation (5):

$$\phi(x) = A_1 \cos ax + A_2 \sin ax + A_3 \cosh ax + A_4 \sinh ax \quad (12)$$

and setting its determinant to zero, or by using equations (9-10) [15].

2.2.2 The closed crack eigenvalue problem

When crack closes, the beam is treated as one continuous Euler-Bernoulli beam and the first mode shape equation is:

$$0 < x < L \rightarrow \phi(x) = \sqrt{\frac{2}{L}} sin(ax) \quad (13)$$

Since the displacement at supports equals zero, the equation (12) is satisfied when *sin (aL)=0*, therefore the natural frequencies of the beam when crack is closed are:

$$\omega_j = j^2\pi^2\sqrt{\frac{EI}{mL^4}}; \quad j = 1, 2, 3, \ldots \quad (14)$$

2.3 Equation of motion of vehicle

The equation of motion of the vehicle, represented as a single degree of freedom oscillator can be represented as

$$m_V\ddot{z} + K[z - r(vt) - y(vt, t)] = 0 \quad (15)$$

2.4 Surface roughness

From ISO 8606:1995(E) [26] specifications RSR function $r(\bar{x})$ in discrete form is:

$$r(\hat{x}) = \sum_{k=1}^{N} \sqrt{4S_d(f_0)\left(\frac{2\pi k}{L_c f_0}\right)^{-2}\frac{2\pi}{L_c}} cos\left(\frac{2\pi k f_0}{L_c} + \theta_k\right) \quad (16)$$

here $S_d(f_0)$ is roughness coefficient; $f_0 = 1/2\pi$ is the discontinuity frequency; L_c is twice the length of the bridge [6, 28]; N is number of data points of successive ordinates of surface profile; and θ_k is a set of independent random phase angles uniformly distributed between 0 and 2π. The road classification according to ISO 8606:1995(E) is based on value of $S_d(f_0)$. Five classes of road surface roughness representing different qualities of the road surface are A (very good), B (good), C (average), D (poor), E (very poor) with value of roughness coefficients 6×10^6, 16×10^6, 64×10^6, 256×10^6, and 1024×10^6 m^3/cycle, respectively. Typical irregular surface roughness profiles are shown in Figure 2.

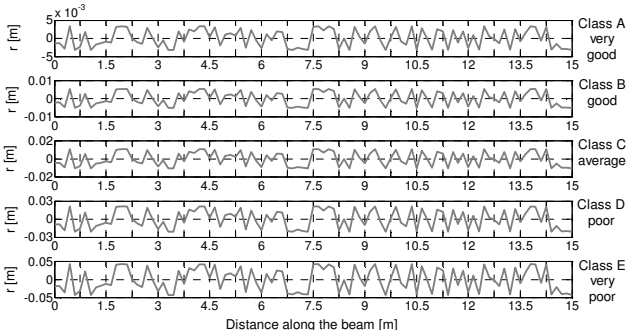

Figure 2: Typical road surface profiles

2.5 Damaged Beam – Moving Oscillator Interaction Including Surface Roughness

The bridge-vehicle interaction can finally be expressed as a system of two second order equations. For a first mode shape consideration (subscripted 1), equations (1) and (15) can be written in matrix form as

$$\begin{bmatrix}1 & 0\\ 0 & 1\end{bmatrix} \times \begin{Bmatrix}\ddot{q}_1\\ \ddot{z}\end{Bmatrix} + \begin{bmatrix}2\xi_1\omega_1 & 0\\ 0 & 0\end{bmatrix} \times \begin{Bmatrix}\dot{q}_1\\ \dot{z}\end{Bmatrix} + \begin{bmatrix}\omega_1^2 - \frac{K}{\rho A}\phi_1(vt)\phi_1(vt) & \frac{K}{\rho A}\phi_1(vt)\\ -\omega_V^2\phi_1(vt) & \omega_V^2\end{bmatrix} \times \begin{Bmatrix}q_1\\ z\end{Bmatrix} = \begin{Bmatrix}\frac{m_V g}{\rho A}\phi_1(vt) + \frac{K}{\rho A}r(vt)\phi_1(vt)\\ \omega_V^2 r(vt)\end{Bmatrix} \quad (17)$$

Where the natural frequency of vehicle is $\omega_V^2 = K/m_V$; and ξ and ξ_v are damping ratio of bridge and vehicle, respectively. The displacements and velocities of the beam and the vehicle are obtained by using a 4/5th order Runge-Kutta method available in MATLAB [29].

3 DAMAGE DETECTION THROUGH SURFACE ROUGHNESS

The proposed concept of numerical analysis is shown in Figure 3.

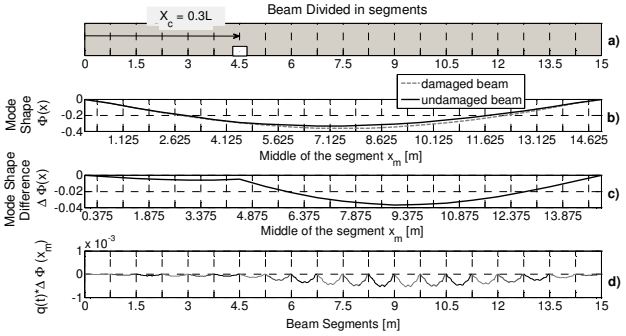

Figure 3: a) Simply supported beam with damage located at 0.3L divided into equal segments; b) Mode shape of damaged and undamaged beam; c) Difference in mode shape of undamaged and damaged beam; d) Difference in mode shape of damaged and undamaged beam at mid location of each segment multiplied with temporal beam displacement.

The beam is divided into a number of equal segments. In this example (Figure 3b) the crack is located at $x_c = 0.3L$. The difference between the damaged and undamaged mode shapes is found next ($\Delta\Phi_m$), which has a local maximum and discontinuous slope at the damage location [27]. In practice, the mode shape difference in the spatial domain is hard to detect. For an experimental regime, an initial estimate of the undamaged mode shape and natural frequency should be carried out and the bridge response obtained is used to create a difference function in the time domain as $\Delta\Phi_m q(t)$. This is not implicit but explicit as in reality the bridge responses may be measured at multiple locations. The response at different locations are scaled proportional to the first damaged modeshape with respect to the maximum value of the modeshape. Random white noise is cancelled out by considering the passage of many vehicles and the

consideration of normalisation. When a coloured noise is present in bridge response than the damage might not identified due if the masking effect is high. Figure 3 shows that the location near the damage is affected in this differenced time domain response. The location of the damage(s) could be indicated by using wavelet analysis as shown in many papers [30-32]

The data used for the bridge model are L = 15m; modal damping ratio of the beam ζ = 2%; E = 200e9 N/m^2 and ρ = 7900 kg/m^3. The static deflection of the beam is 0.005 m based on this data. It is assumed that that the depth (h) of the beam is 1.5 times the width (b) of the beam. Other geometric descriptors like second moment of area (I), h, b, cross sectional area (A) and m are computed based on this assumption. The data used for vehicle simulation are m_v = 3000 kg and K = 3.65e6 N/m [6, 33]. The calculated natural frequencies of bridge without damage and vehicle are 4Hz and 2Hz respectively. The geometry of the equivalent beam is thus reflected in the actual guiding values of the response parameters of the bridge.

Choice of Damage Detection and Calibration Markers

Statistical descriptors on previously determined functions $\Delta\Phi_m q(t)$ for each segment of the beam are observed and investigated for monotonocity and consistency. The statistical parameters of function $\Delta\Phi_m q(t)$ considered included mean (μ), standard deviation (σ), skewness (λ), and kurtosis (κ). The choice of mean and standard deviation stemmed out of the recent study [25]. The parameters are computed as follows:

$$\mu = \frac{1}{m}\sum_{i=1}^{m} x_i \tag{18}$$

$$\sigma = \sqrt{\frac{1}{m}\sum_{i=1}^{m}(x_i - \mu)^2} \tag{19}$$

Figure 4 shows an example of mean and standard deviation of $\Delta\Phi_m q(t)$ function calculated for each beam segment. It is found that obtained mean and standard deviation functions are similar in shape and clearly show the discontinuous slope at the damage location, similar to mode shape difference functions. This finding is consistent with [25] where it has been proven that first and second order cumulants of bilinear and linear system response are consistent and monotonic descriptors of the system characteristics and are sensitive to system stiffness changes.

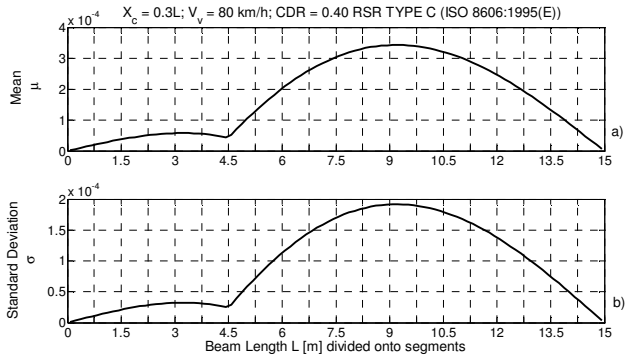

Figure 4: Example of calculated: a) Mean and b) Standard Deviation (STD) for crack located at Xc = 0.3L; Speed of the vehicle Vv = 80km/h; Crack Depth Ratio CDR = 0.40 and Type C Road Surface Roughness (RSR) defined as per ISO 8606:1995(E).

4 DISCUSSION

Figure 5 represents an example of mean and standard deviation functions for the case of different road surface roughness (A to E) where the crack is located at quarter-span, the vehicle is moving with a speed 80km/h and crack depth ratio is 0.4. From this and the similar figures obtained by varying x_c, CDR and V_V, a number of observations are noted. It is observed that the markers μ and σ show kink at the damage location, values of statistical parameters relative to each other increase with decreasing road quality and μ and σ curves slope discontinuity at the crack location become more obvious for poor and very poor grades of road surface roughness. All of the above indicate that the location of crack can be identified by the chosen markers and that consistent calibration is possible.

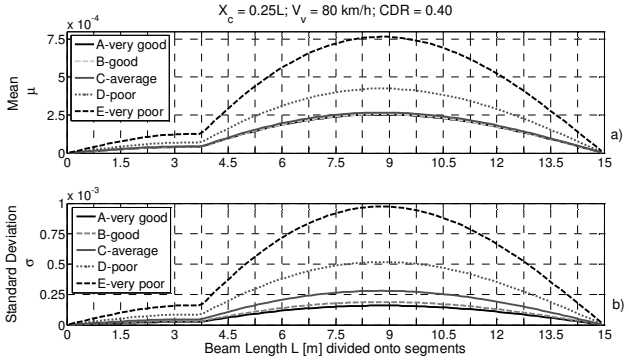

Figure 5: a) Mean and b) Standard Deviation (STD) for crack located at Xc = 0.25L; Speed of the vehicle Vv = 80km/h; Crack Depth Ratio CDR = 0.40, and different types of Road Surface Roughness (RSR) defined as per ISO 8606:1995(E).

For illustration purposes, Figures 5, 6 and 7 representing standard deviation in relation to crack depth ratio and vehicle speed for RSR type C for case when crack is located at the edge, quarter-span and mid-span of the beam, respectively, are shown.

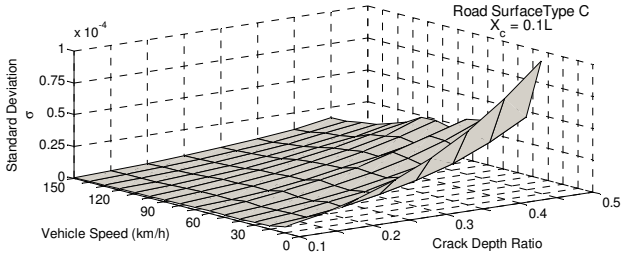

Figure 6: Standard deviation dependence on Crack Depth Ratio and Vehicle speed for Road Surface Roughness Type C for crack located near support

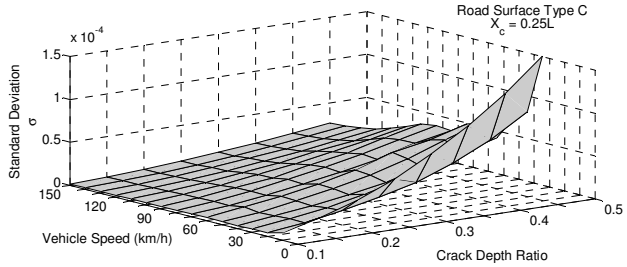

Figure 7: Standard deviation dependence on Crack Depth Ratio and Vehicle speed for Road Surface Roughness Type C for crack located at quarter-span

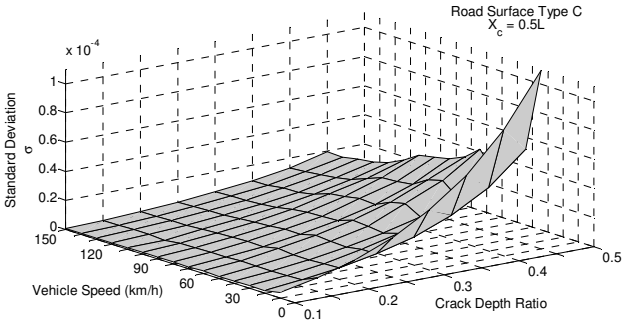

Figure 8: Standard deviation dependence on Crack Depth Ratio and Vehicle speed for Road Surface Roughness Type C for crack located at mid-span

In general, it is observed that the relation between μ and σ and CDR for different V_V increases exponentially.

It is noted that these curves are separated into 4 groups depending on V_V: very low speed 10km/h; low speed 20 to 60 km/h; medium speed 70 to 100km/h; and high speed 110 to 150km/h for which variation of μ and σ is very high, high, medium, and low, respectively.

This grouping becomes more obvious for higher CDR when RSR is type D and E, while for the RSR type A and B there is very little difference between statistical parameters even for a higher values of CDR.

The exception is very low V_V for which statistical parameters are observed to be much higher than for other V_V for all cases of RSR. RSR type C and V_V = 80km/h are found to be optimal for calibration purposes. In general, calibrations are monotonic (μ and σ increase with CDR) but there is no obvious relation between the curves representing different crack locations.

Figure 8 shows a generic fit, i.e the calibration of standard deviation in the function of CDR for three different vehicle speeds (low, medium, and high), analysed separately for three different positions of the crack.

The best fit is represented by power equations:

$$\sigma = a \times CDR^b + c \tag{22}$$

The coeficients of fitting functions are given in Table 1.

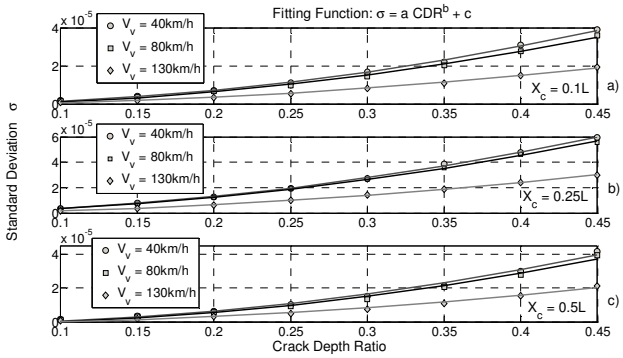

Figure 9: Calibration of Standard Deviation (STD) variation in function Crack Depth Ratio (CDR); for Low, Medium and High Vehicle Speed (Vv) and three different positions of the damage: a) Edge; b) Quarter-span and c) Mid-span.

Table 1. Calibration function for Standard deviation and CDR

Position of the crack	Vehicle speed (km/h)	a	b	c
0.1L	40	1.925e-4	1.997	-4.74e-7
	80	1.756e-4	1.986	-7.94e-7
	130	8.9e-5	1.899	-6.13e-7
0.25L	40	2.747e-4	1.916	4.194e-7
	80	2.629e-4	1.935	6.323e-7
	130	1.353e-4	1.88	-7.43e-8
0.5L	40	2.072e-4	2.022	-1.59e-6
	80	2.058e-4	2.091	-1.48e-6
	130	1.084e-4	2.053	-8.13e-7

5 CONCLUSIONS

The effects of road quality on bridge-vehicle interaction based surface roughness are investigated. In practice the response, displacements and / or velocities (or the first modeshape and its time derivative)can be measured at multiple locations along the bridge. The undamaged responses may be estimated through computation or finite element modelling. The responses of the damaged condition measured at different locations are expected to be scaled approximately with respect to the maximum value. This maximum value does not change too much from the undamaged maximum since local damage affects global responses very little. Estimated damaged modeshape values at different locations can be obtained by dividing the time domain responses at each location by the time domain response at the modeshape maximum value. It is also possible to estimate the time domain response at the maximum modeshape value by dividing the response by the normalising value of integral of the squared modeshape. As long as the masking effects from noise and errors are lower than the local disturbance due to damage, the difference in this scaled time domain response will manifest local distortions in the space domain. It is important to note here that the local response itself is continuous, the derivative is discontinuous, while the second and the third derivatives are continous again in the space domain to ensure moment and shear transfer.

The mean and standard deviation of mode shape differenced temporal responses can be used as damage detection markers. Discontinuous slopes of mean and standard deviation curves give the position of damage, and the jump size is related to the damage extent.

When the road quality decreases, the slope discontinuity of mean and standard deviation curves at the crack location become more obvious. This is amplified for poor and very poor grades of road surface roughness.

The consistency of calibration depends on vehicle speed and road surface type. This is more pronounced in the case of higher damage. Damage calibration on better roads is less uncertain and gives consistent but less sensitive results. Worse roads are less consistent in calibration values but give more sensitive results. Therefore the road surface roughness type C is optimal for calibration purposes.

The study is particularly useful for continuous online bridge health monitoring since the data necessary for analysis can be obtained from the operating condition of the bridge and the structure does not therefore need be closed down.

ACKNOWLEDGMENTS

The Irish Research Council.

REFERENCES

[1] Kisa, M. (2004), 'Free vibration analysis of a cantilever composite beam with multiple cracks', *Composites Science and Technology*, 64 (9), 1391–1402.

[2] Rucka, M. and Wilde, K. (2006), 'Crack identification using wavelets on experimental static deflection profiles', *Engineering Structures*, 28 (2), 279–288.

[3] Pakrashi, V., O'Connor, A., Breysse, D. and Schoefs, F. (2008), 'Reliability Based Assessment of Structures in Marine Environment', *MEDACHS 08 Conference on Construction Heritage in Coastal and Marine Environments*, Lisbon, Portugal

[4] Pakrashi, V., O'Connor, A. and Basu, B. (2010), 'A Bridge–Vehicle Interaction Based Experimental Investigation of Damage Evolution', *Structural Health Monitoring*, 9 (4), 285 - 296.

[5] Delgado, R. M. and dos Santos, R. C. S. M. (1997), 'Modelling of a railway bridge–vehicle interaction on high speed tracks', *Computers and Structures*, 63 (3), 511-523

[6] Henchi, K., Fafard, M., Talbot, M. and Dhatt, G. (1998), 'An Efficient Algorthm for Dynamic Analysis of Bridges under Moving Vehicles Using a Coupled Modal and Physical Components Aproach', *Journal of Sound and Vibration*, 212 (4), 663-683

[7] Bilello, C., Bergman, A. L. and Kuchma, D. (2004), 'Experimental investigation of a small-scale bridge model under a moving mass', *ASCE Journal of Structural Engineering*, 130 (5), 799–804.

[8] Bilello, C. and Bergman, L. A. (2004), 'Vibration of damaged beams under a moving mass: Theory and experimental validation', *Journal of Sound and Vibration*, 274 (3-5), 567–582.

[9] Bu, J. Q., Law, S. S. and Zhu, X. Q. (2006), 'Innovative bridge condition assessment from dynamic response of a passing vehicle', *ASCE Journal of Engineering Mechanics*, 132 (12), 1372–1379.

[10] Majumder, L. and Manohar, C. S. (2003), 'A time domain approach for damage detection in beam structures using vibration data with a moving oscillator as an excitation source. ', *Journal of Sound and Vibration*, 268 699–716.

[11] Lee, J. W., Kim, J. D., Yun, C. B., Yi, J. H. and Shim, J. M. (2002), 'Health monitoring method for bridges under ordinary traffic loadings', *Journal of Sound and Vibration*, 257 (2), 247–264.

[12] Law, S. S. and Zhu, X. Q. (2005), 'Bridge dynamic responses due to road surface roughness and braking of vehicle', *Journal of Sound and Vibration*, 282 (3-5), 805-830

[13] Friswell, M. I. and Penny, J. E. T. (2002), 'Crack Modeling for Structural Health Monitoring', *Structural Health Monitoring*, 1 (2), 139 - 148.

[14] Narkis, Y. (1994), 'Identification of crack Location in vibrating simply supported beams', *Journal of sound and Vibrations*, 172 (4), Pages 549-558

[15] Sundermeyer, J. N. and Weaver, R. L. (1994), 'On Crack Identification and Characterization in a beam by non-linear vibration analysis', *Journal of Sound and Vibration*, 183 (5), 857-871.

[16] Harris, N. K., Gonzalez, A., Obrien, E. J. and McGetrick, P. (2010), 'Characterisation of pavement profile heights using accelerometer readings and a combinatorial optimisation technique', *Journal of Sound and Vibration*, 329 (5), 497-508.

[17] Fryba, L., *Vibration of Solids and Structures under Moving Loads*, Publishing house of Academy of Sciences of the Czech Republic, Thomas Telford Ltd., Prague, London, 3rd edition, 1999.

[18] Abdel-Rohman, M. and Al-Duaij, J. (1996), 'Dynamic Response of Hinged-Hinged Single Span Bridges with Uneven Deck', *Compurers & Structures1996*, 59 (2), 291-299.

[19] O'Brien, E., Li , Y. and Gonzalez, A. (2006), 'Bridge roughness index as an indicator of bridge dynamic amplification', *Compurers & Structures*, Volume 84 (12), 759–769.

[20] da Silva, J. G. S. (2004), 'Dynamical performance of highway bridge decks with irregular pavement surface', *Computers & Structures*, 82 (11-12), 871-881

[21] Sohn, H., Farrar, C. R., Hunter, N. F. and Worden, K. (2001), 'Structural Health Monitoring using Statistical Pattern Recognition Techniques', *ASME Journal of Dynamic Systems, Measurement and Control* 123 (4), 706-717.

[22] Pakrashi, V., Basu, B. and Connor, A. O. (2009), 'A Statistical Measure for Wavelet Based Singularity Detection', *Journal of Vibration and Acoustics*, 131 (4), 041015 (6 pages)

[23] Cacciola, P., Impollonia, N. and Muscolino, G. (2003), 'Crack detection and location in a damaged beam vibrating under white noise', *Computers and Structures*, 81 1773–1782.

[24] Hadjileontiadis, L. J., Douka, E. and Trochidis, A. (2005), 'Crack Detection in Beams using Kurtosis', *Computers and Structures*, 83 909-919.

[25] Jaksic, V., Pakrashi, V. and O'Connor, A. (2011), 'Employing Surface Roughness for Bridge-Vehicle Interaction based damage detection', *ASME 2011 International Mechanical Engineering Congress and Exposition (IMECE 2011)* Denver, Colorado, USA,

[26] *ISO 8606:1995(E). Mechanical vibration - road surface profiles-reporting of measured data*, 1995.

[27] Poudel, U. P., Fu, G. and Ye, J. (2005), 'Structural damage detection using digital video imaging technique and wavelet transformation', *Journal of Sound and Vibration*, 286 (4-5), 869–895.

[28] Wu, S. Q. and Law, S. S. (2011), 'Vehicle axle load identification on bridge deck with irregular road surface profile', *Engineering Structures*, 33 (2), 591-601

[29] MATLAB 7, 2004. The MathWorks, Inc., Natick, MA.

[30] Chang, C.-C. and Chen, L.-W. (2003), 'Vibration damage detection of a Timoshenko beam by spatial wavelet based approach ', *Applied Acoustics*, 64 (12), 1217-1240

[31] Okafor, A. C. and Dutta, A. (2000), 'Structural damage detection in beams by wavelet transforms', *Smart Materials and Structures*, 9 (6), 906–917.

[32] Loutridis, S., Doukab, E. and Trochidis, A. (2004), 'Crack identification in double-cracked beams using wavelet analysis ', *Journal of Sound and Vibration*, 277 (4-5), 1025-1039